Open Access
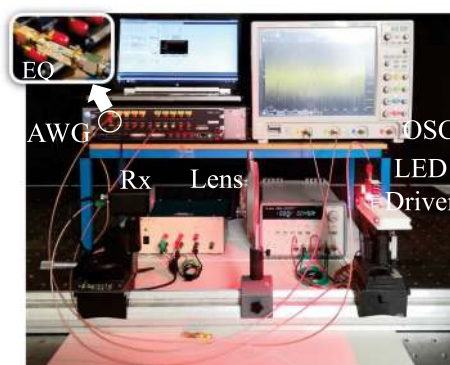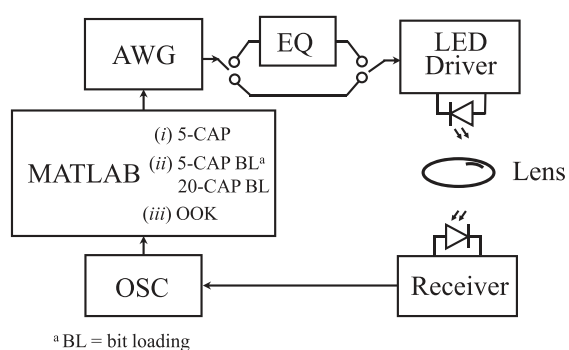
Should Analogue Pre-Equalisers be Avoided in VLC Systems?

Xicong Li
Zabih Ghassemlooy
Stanislav Zvanovec
Rafael Perez-Jimenez
Paul Anthony Haigh

photonics SOCIETY

IEEE

Should Analogue Pre-Equalisers be Avoided in VLC Systems?

Xicong Li [ORCID],[1] **Zabih Ghassemlooy** [ORCID],[1] **Stanislav Zvanovec** [ORCID],[2]
Rafael Perez-Jimenez,[3] **and Paul Anthony Haigh** [ORCID] [4]

[1]Optical Communications Research Group, Northumbria University, Newcastle upon Tyne, NE1 8ST, U.K.
[2]Department of Electromagnetic Field, Faculty of Electrical Engineering, Czech Technical University in Prague, Prague 16627, Czech Republic
[3]IDeTIC, University of Las Palmas de Gran Canaria, Las Palmas de Gran Canaria, 35017, Spain
[4]Intelligent Sensing and Communications Group, Newcastle University, Newcastle upon Tyne, NE1 7RU, U.K.

Abstract: Visible light communication (VLC) systems are highly constrained by the limited 3-dB bandwidth of light-emitting diodes (LEDs). Analogue pre-equalisers have been proposed to extend the LED's bandwidth at the cost of reduced signal-to-noise ratio (SNR). Compared with the pre-equaliser, the multi-carrier modulation with bit-loading can efficiently use the spectrum beyond the LED's raw 3-dB bandwidth without incuring SNR penalties by employing multiple narrow quasi-flat sub-bands to eliminate the need for equalisation. In this work we show by means of theoretical and experimental investigation that VLC with multi-band carrierless amplitude and phase modulation with bit-loading can outperform VLC with analogue pre-equalisers.

Index Terms: Visible light communications (VLC), channel capacity, equaliser, CAP.

1. Introduction

Visible light communications (VLC) have attracted intensive research interests due to its capability to provide multiple functionalities of illumination, data communications, sensing and indoor localisation [1], [2]. In VLC systems, both laser and light-emitting diodes (LEDs) could be used as the transmitter. The former offers higher modulation bandwidth at the expense of high directionality and increased cost when used for indoor lighting [3]–[5]. Note that future lighting infrastructure may use the white laser, therefore opening up the potential for high-speed laser-based VLC. Whereas, LEDs are widely used for illumination in indoor and outdoor applications, and therefore can be effectively utilised for data communications with minor modifications to existing lighting and power line infrastructures to reduce the deployment cost. However, LED-based VLC systems are highly constrained by the low modulation bandwidth B_{mod} of LEDs used for general-purpose illumination due to the large areas (i.e., high capacitance). Off-the-shelf single colour LEDs have a B_{mod} of several MHz, while white phosphorous LEDs based on blue LEDs coated with a Ce:YAG

colour converting phosphor have even lower B_{mod} because of the slow temporal response of the phosphor [6], [7].

To address the modulation bandwidth problem and to extend the system data throughput, many schemes including multi-level modulation, multi-carrier modulation and analogue pre- and post-equalisers have been investigated [8]–[14]. In [11], a first-order post-equaliser (post-EQ) was used at the receiver (Rx) to compensate for the frequency response of the blue component of a white phosphorous LED, to increase B_{mod} from 10 MHz (the blue component bandwidth) to 50 MHz. Using a lens and a blue filter, 100 Mbit/s on-off keying (OOK) data was transmitted over a distance of 10 cm. In [12], a pre-equaliser (pre-EQ) with an emitter degenerated LED driver and a post-EQ were adopted to achieve 662, 600, 520 Mbit/s OOK transmission using blue (B), red (R) and green (G) LEDs separately. The bandwidth was improved from 6 (R), 5 (G) and 5 (B) MHz to 112 (R), 92 (G), 103 (B) MHz using a pre-EQ only and to 180 (R), 185 (G), 150 (B) MHz with pre- and post-EQs. In [13], the VLC system bandwidth was increased from 38 to 79 and 366 MHz using one- and two-stage bridge-T pre-EQs, respectively, where 16-quadrature amplitude modulation (16-QAM) orthogonal frequency division multiplexing (OFDM) was employed to achieve a data transmission rate of 1.6 Gb/s. The bridge-T structure, which was first introduced for copper telephone lines to deliver high-quality voice transmission [15], has a constant impedance [16], [17], thus facilitating impedance matching. Note that LEDs have a rather low impedance (few ohms including the parasitic resistance) when biased at high currents [18], and therefore cannot be directly connected to the bridge-T equaliser. In [14], both active pre- and post-EQs were used to increase the bandwidth from 12 to 233 MHz in order to transmit 550 Mb/s OOK data. However, there are issues within the work in [14]. Although active components were used in the pre-EQ, signal amplification was not introduced to improve the signal-to-noise ratio (SNR). This is because a small input signal level was used to avoid clipping distortion due to the limited headroom at the equaliser's output and the high gain of the two-stage amplification. Therefore, in terms of the frequency response, the active two-stage pre-EQ can be considered as a second-order high pass filter. The post-EQ provides higher gain at high frequencies thus leading to increased noise floor, which is not desirable.

To summarise, the pre-EQ improves B_{mod} of the LED at the cost of reduced modulation depth [12], [13], [19], while the post-EQ improves B_{mod} at the cost of the increased noise level [11], [19]. In other words, the analogue equaliser extends B_{mod} by sacrificing SNR. However, bandwidth is only part of the story as Shannon's capacity theorem [20] states that the system capacity is determined by the product of bandwidth B_{mod} and spectrum efficiency η_{se}. Although increased VLC system data rates with analogue equalisers have been extensively reported in the literature as introduced previously, few have compared the system performance employing equalisers with the raw system without any SNR penalties. Compared with equalised systems, the raw system has higher SNR and thus can achieve higher η_{se} by adopting multi-level and multi-carrier modulation, where the full band is divided into a number of narrow sub-bands with an almost flat response to eliminate the need for equalisers. Due to the absence of an SNR penalty, the raw system can load more bits onto each sub-band using bit-loading algorithms to achieve the optimum spectrum efficiency performance [9]. Therefore, the raw system with multi-carrier modulation and bit-loading can outperform equalised systems [21].

Experimental reports have demonstrated VLC systems with analogue pre-equalisation in conjunction with bit-loading [22]. However the transmission gains of each channel are normalised to the maximum, and hence, the SNR penalty of the analogue pre-equaliser is not readily known. Furthermore, after equalisation, the transmission experiments are performed, but only consider a varying distance, and are never compared with the raw system response without the pre-equaliser. This paper fills that gap by investigating several pre-equaliser designs in comparison to a raw system performance with no equaliser.

In this paper, we have adopted the multi-band carrier-less amplitude phase modulation (*m*-CAP) as the multi-carrier scheme because of its simple implementation and high η_{se} [23]. The results confirm that *m*-CAP with bit-loading can outperform the equalised VLC system for the links under

test. However, the analogue pre-equaliser can be used as an efficient alternative to improve the system data rate with low implementation complexity compared with m-CAP with bit-loading.

The remainder of the paper is organised as follows. Section 2 proposes a complete system model with the analogue pre-equaliser and investigate the effect of the analogue pre-equalise on VLC system capacity. Section 3 demonstrates how to design the pre-equaliser for a red high-power LED (OSRAM LR W5SM) with a raw B_{mod} of 7.5 MHz using the method introduced in Section 2. For the reason of simplicity, we choose a single colour LED to avoid the effect of the phosphor [6]. Section 4 to 6 provide a comparison of the performance of systems with and without equalisers. For the raw system without equalisers, the multi-carrier modulation with the bit-loading algorithm is adopted to explore the maximal data rates of the raw system. Finally, Section 7 concludes the paper.

2. VLC With Analogue Pre-Equalisers

In this section, we first introduce the constraints that a VLC system with the analogue equaliser has to follow from a practical point of view.[1] Then a thorough system model and an analogue equaliser design method are proposed.

2.1 System Constraints

Constraint 1 (The analogue pre-equaliser is a lossy system): This constraint is because of the inherent limited dynamic range of an LED or the maximum achievable dynamic range of a practical LED driver. For an LED with a particular bias current I_b, the maximum modulation current (ac part) range must meet $|i_T(t)| \leq I_b$. For a practical LED driver, the dynamic range of $i_T(t)$ will be limited by hardware implementation, i.e. $|i_T(t)| \leq mI_b$, where $m = \frac{\max|i_T(t)|}{I_b}$ is the modulation depth. Imagine a system with a driver which can provide a maximum modulation current range $\max|i_T(t)| = I_b$. Such a system will offer the best SNR with a modulation depth of 100%. In order to realise high frequency emphasis for equalisation in such a system, the analogue pre-equaliser has to introduce attenuation at low frequencies.[2]

Constraint 2 (The VLC system is power limited): The second constraint is the straightforward derivation from the previous discussion. Since $|i_T(t)| \leq mI_b$, the average optical power of the modulated ac signal follows

$$\lim_{T \to \infty} \frac{1}{T} \int_{-T/2}^{T/2} \eta_{eo}|i_T(t)|\, dt \leq \eta_{eo}mI_b, \tag{1}$$

where η_{eo} is the electrical-to-optical efficiency.

2.2 System Modeling

Considering above constraints, we propose a model for a VLC system with an analogue equaliser as shown in Fig. 1 consisting of a signal generator, an equaliser (optional), an LED driver (shown as a voltage-controlled current source, i.e. VCCS), an LED, a photodiode and a transimpedance amplifier (TIA). If not stated, all the functions starting with small initials represent the AC signal. The analysis also applies to the dc signal but with different parameter values.

At the transmitter, the signal generator with an output resistance R_0 (normally 50 Ω) is connected to the LED driver through an optional equaliser. Here the purpose of the driver is to turn the LED from current driving to voltage driving and to provide impedance conversion for the ease of the

---

[1]We neglect nonlinearity in this paper.

[2]The reader may ask why not use an amplifier to compensate for the signal attenuation caused by the equaliser [13] Normally, the use of amplifier increases the LED's modulation current $i_T(t)$ and therefore modulation depth m. If you do use an amplifier after the analogue equaliser, the average power (ac part, this is defined in a similar way as optical modulation amplitude in fiber communication [24]) is also increased. Therefore, the use of amplifier or active components do not alter the nature of the analogue equaliser from a system perspective.
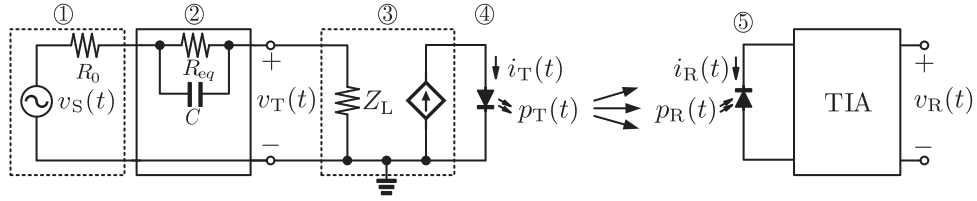
Fig. 1. System block diagram of a VLC system with (1) signal source, (2) equaliser, (3) voltage controlled current source, (4) LED, (5) photodiode and TIA receiver.

equaliser design.[3] Considering the LED as a first-order system, an equaliser based on an RC high-pass filter is adopted. Assuming the driver is designed with $Z_L = R_0$, we can obtain the transfer function of the equaliser

$$H_{EQ}(s) = \frac{V_T(s)}{V_S(s)} = \frac{R_0}{2R_0 + R_{eq}} \frac{1 + \frac{s}{R_{eq}C}}{1 + \frac{s}{(2R_0//R_{eq})C}}, \tag{2}$$

where $V_T(s)$ and $V_S(s)$ are the Laplace transform of $v_T(t)$ and $v_S(t)$, respectively. Since $v_T(t)$ is the voltage that controls the current through the LED, we have

$$i_T(t) = \eta_{mod} v_T(t), \tag{3}$$

where η_{mod} is the transconductance of the VCCS driver. Therefore, the corresponding output optical power is

$$p_T(t) = \eta_{eo} i_T(t) \circledast h_{LED}(t), \tag{4}$$

where $\circledast$ denotes time-domain convolution, $h_{LED}(t)$ is the LED's impulse response and its Laplace transform is given by [25]

$$H_{LED}(s) = \frac{1}{1 + \frac{s}{\omega_{LED}}}, \tag{5}$$

where $\omega_{LED} = 2\pi f_{3dB}$, and f_{3dB} is the 3-dB bandwidth of the LED.

At the receiver, for a line-of-sight link, the received optical power at the photodiode is [1]

$$p_R(t) = H_{ch}^2(0) p_T(t), \tag{6}$$

where $H_{ch}^2(0)$ is the channel gain coefficient in the optical domain. Then the detected current and corresponding voltage signal can be caculated by

$$i_R(t) = R \cdot p_R(t), \tag{7}$$

$$v_R(t) = G_{ac} i_R(t), \tag{8}$$

where R is the responsibility of the photodiode and G_{ac} is the AC gain of the TIA.

Using (3) to (8), we can rewrite the recovered voltage as follows

$$v_R(t) = G_{ac} R H_{ch}^2(0) \eta_{eo} \eta_{mod} v_T(t) \circledast h_{LED}(t). \tag{9}$$

Applying Laplace transform to (9), the frequency response of the VLC system becomes

$$H_{VLC}(s) = \frac{V_R(s)}{V_T(s)} = A_0 H_{LED}(s), \tag{10}$$

[3]When a bias-tee is used as an LED driver, Z_L then equals the LED's impedance and is not a resistive load [18]. Designing an equaliser with the target impedance Z_L is essentially an impedance matching problem and is much more challenging due to the LED's low resistive impedance and the need of wideband impedance matching.
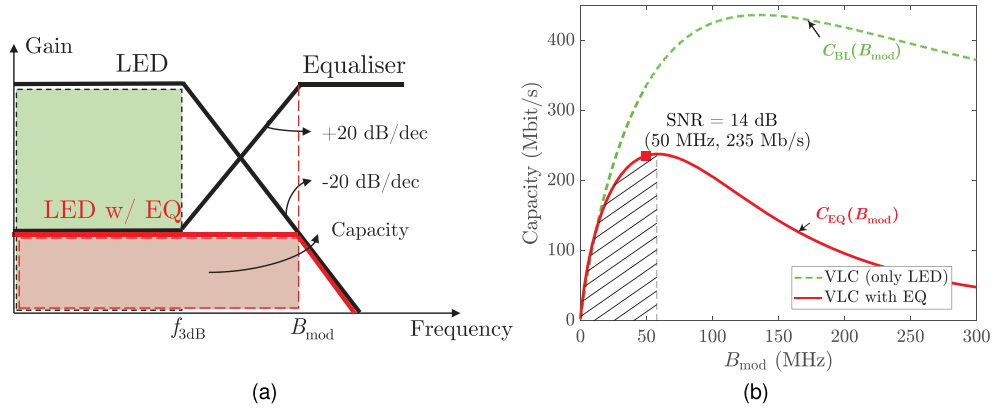
Fig. 2. (a) Frequency response of the LED and the equaliser and (b) the capacity vs. B_{mod} with $f_{3dB} = 10$ MHz and $SNR(f) = 35$ dB for $0 < f < f_{3dB}$.

where $A_0 = G_{ac}RH_{ch}^2(0)\eta_{eo}\eta_{mod}$. Using (2) and (10), we can get the frequency response of the entire system

$$H_{VLC+EQ}(s) = \frac{V_R(s)}{V_T(s)}\frac{V_T(s)}{V_S(s)} = \frac{A_0R_0}{2R_0+R_{eq}}\frac{1+\frac{s}{R_{eq}C}}{1+\frac{s}{(2R_0//R_{eq})C}}\frac{1}{1+\frac{s}{\omega_{LED}}}. \tag{11}$$

If let $R_{eq} = 0$, (11) degrades to the raw VLC system without equaliser.[4] Fig. 2(a) shows the frequency response of (2), (10) and (11) using bode plots. To achieve equalisation, the zero in (2) must equal the pole in (10) to cancel each other, i.e.,

$$\omega_{LED} = 2\pi f_{3dB} = \frac{1}{R_{eq}C}. \tag{12}$$

Equation (12) is the key criterion for the analogue equaliser design. With (12) satisfied, the equalised VLC system then has the frequency response of

$$H_{VLC+EQ}(s) = \frac{A_0R_0}{2R_0+R_{eq}}\frac{1}{1+\frac{s}{(2R_0//R_{eq})C}}, \tag{13}$$

indicating a bandwidth increase from $f_{3dB} = \frac{1}{2\pi R_{eq}C}$ to $B_{mod} = \frac{1}{2\pi(2R_0//R_{eq})C}$ at the cost of reduced power level from $(\frac{A_0}{2})^2$ to $(\frac{A_0R_0}{2R_0+R_{eq}})^2$. Here we define the gain-bandwidth product GBP $= \frac{A_0 \cdot f_{3dB}}{2}$.

2.3 Capacity Analysis

This subsection aims to investigate the effect of a lossy pre-equaliser on the system's capacity. Although employing analogue equalisers to increase data rates of VLC systems has been widely reported in the literature, the underlying principle has not been studied. As discussed previously, the analogue equaliser extends the system's 3-dB bandwidth at the cost of reduced signal power which is related to SNR; therefore, we cannot take the increase in the system capacity for granted because the capacity is the product of bandwidth and the logarithm of the SNR.

Prior to carrying on the analysis, we outline the following observation and assumptions:
 i) The full bandwidth is equal to the 3-dB bandwidth of the equalised system, i.e. B_{mod};
 ii) The analogue equaliser results in flat frequency response so that there is no need for power loading over B_{mod};

---

[4]Due to impedance matching between the signal source and the driver, a factor of 0.5 (6 dB loss in the power domain) is introduced.

iii) To obtain the closed-form solution, power loading is not applied to all schemes.

Let $P_s(f)$ denote the power spectrum of the transmit signal $v_S(t)$, and based on the constraint 2 we have[5]

$$\int_0^{B_{mod}} P_S(f)\, df \leq P_{avg}. \tag{14}$$

Based on the assumption (ii), the power is spread evenly over the full bandwidth, so the power spectrum can be approximately estimated by

$$P_S(f) = \frac{P_{avg}}{B_{mod}}. \tag{15}$$

In an additive white Gaussian noise environment with a noise power density of $N(f) = N_0$, the SNR at the Rx can be calculated by

$$\text{SNR}(f) = \frac{P_S(f)}{N(f)} |H_{VLC+EQ}(f)|^2. \tag{16}$$

Therefore, the channel capacity can be given by [20]:

$$C_{EQ}(B_{mod}) = \int_0^{B_{mod}} \log_2\left[1 + \text{SNR}(f)\right] df \tag{17}$$

$$= \int_0^{B_{mod}} \log_2\left[1 + \frac{P_{avg}}{N_0 B_{mod}} \left(\frac{GBP}{B_{mod}}\right)^2 \frac{1}{1 + \left(\frac{f}{B_{mod}}\right)^2}\right] df$$

$$< B_{mod} \log_2\left[1 + \frac{A f_{3dB}^2}{B_{mod}^3}\right], \tag{18}$$

where $A = (A_0^2 P_{avg})/(4N_0)$. As $B_{mod} \to \infty$, $\log_2[1 + \frac{A f_{3dB}^2}{B_{mod}^3}] \to \frac{1}{\ln 2} \frac{A f_{3dB}^2}{B_{mod}^3}$. Thus, $C_{EQ}(B_{mod})$ will approach zero when the normalised 3-dB bandwidth (i.e. B_{mod}) after equalisation goes to infinity. Recalling that $C(B_{mod})$ starts from zero (when $B_{mod} = 0$) and approaches zero when $B_{mod} \to \infty$, there shall be a local maximum to achieve the highest capacity. This explains why the analogue equaliser can increase the system data rate even though SNR penalties are introduced. Additionally, there exists an optimal point to achieve the largest capacity.

Using (18) as the upper bound of $C_{EQ}(B_{mod})$, the capacity is plotted as a function of B_{mod} in Fig. 2(b) with $f_{3dB} = 10$MHz and $\text{SNR}(f) = 35$ dB, $0 < f < f_{3dB}$.[6] The local peak is consistent with the previous discussion. In order to achieve increased system capacity, the equalised bandwidth should fall in the shaded region in Fig. 2(b). One point in the shaded area is highlighted as an example to show that an increased capacity of 235 Mb/s is expected when B_{mod} is extended to 50 MHz at the cost of an SNR penalty of $30\log_{10}(50/10) = 21$dB. In a practical system, the procedure involves optimising all the parameters related to the system gain, including the equaliser gain, VLC channel path loss, and the receiver's TIA gain.

2.4 Higher Capacity Without SNR Penalties: Multi-Carrier Modulation

The disadvantage of using an analogue pre-equaliser is the reduced SNR level, which is obvious that the corresponding capacity is not optimum. There is an alternative option in improving the spectral efficiency based on multi-carrier modulation. In multi-carrier modulation, the full band is

---

[5]P_{avg} in (14) is the corresponding average power in the electrical domain, i.e. $P_{avg} \leq (ml_b/\eta_{mod})^2$.

[6]For comparative purposes, all the parameters adopted here is from our measured data which can be found later in the Fig. 9(a). For the raw VLC system, i.e. 5-CAP with no EQ, we can estimate the SNR by $\text{SNR}(f) = \frac{A_0^2 P_{avg}}{4N_0 f_{3dB}} = \frac{A}{f_{3dB}} = \text{SNR}_0$ for $0 < f < f_{3dB}$. SNR_0 is the measured SNR. Thus, (18) turns to $B_{mod} \log_2\left[1 + \text{SNR}_0 f_{3dB}^3/B_{mod}^3\right]$. Then the curve can be obtained with $\text{SNR}_0 = 10^{35/20}$ and $f_{3dB} = 10$ MHz.
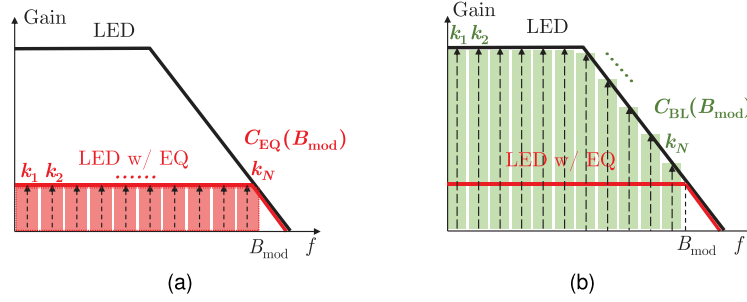
Fig. 3. Illustrative plots for the capacity of a VLC system with: (a) the analogue equaliser and (b) bit-loading.

divided into a number of narrow sub-bands, which can be regarded as quasi-flat and therefore can make the most of SNR by bit-loading with no attenuation. This is best illustrated by Fig. 3, where for the same B_{mod} the multi-carrier modulation with bit-loading always offers higher capacity than the pre-equaliser [21].

The closed-form of the capacity without the analogue equaliser can be derived in the same way as (17)

$$
\begin{aligned}
C_{\text{BL}}(B_{\text{mod}}) &= \int_0^{B_{\text{mod}}} \log_2 \left[1 + \frac{A_0^2 P_{\text{avg}}}{4 N_0 B_{\text{mod}}} \frac{1}{1 + \left(\frac{f}{f_{\text{3dB}}}\right)^2} \right] df \\
&= \frac{f_{\text{3dB}}}{\ln 2} \left[\frac{B_{\text{mod}}}{f_{\text{3dB}}} \ln \left[1 + \frac{A}{B_{\text{mod}} \left(1 + \frac{B_{\text{mod}}}{f_{\text{3dB}}}^2 \right)} \right] - 2 \tan^{-1} \left(\frac{B_{\text{mod}}}{f_{\text{3dB}}} \right) \right. \\
&\left. + 2 \sqrt{1 + \frac{A}{B_{\text{mod}}}} \tan^{-1} \left(\frac{B_{\text{mod}}}{f_{\text{3dB}} \sqrt{1 + \frac{A}{B_{\text{mod}}}}} \right) \right],
\end{aligned}
\tag{19}
$$

Similarly, $C_{\text{BL}}(B_{\text{mod}}) \to 0$ with $B_{\text{mod}} \to \infty$, indicating the existence of an optimum point to reach the maximum capacity. The corresponding curve given in Fig. 2(b) is plotted with the same parameter $A = \text{SNR}_0 \cdot f_{\text{3dB}}$ as in (18) and is in a good agreement with the analysis.

To conclude, for a VLC system with the first-order response, there always exists an optimum modulation bandwidth to achieve a maximum capacity under the condition of a limited transmit power and no power-loading.

3. Analogue Pre-Equaliser Design
3.1 LED Current Driver Design

When including a pre-equaliser at the transmitter, one must consider the impedance mismatch issue when driving the LED, which has a dynamic resistance of less than 5 Ω at a high bias current level [18], with a standard 50 Ω signal generator. Fig. 4(a) shows the Tx schematic which consists of a signal generator with the output impedance $R_0 = 50$ Ω, an equaliser, and a MOSFET-based voltage to current LED driver [24] for intensity modulation of the LED. The measured drain current I_{LED} as a function of the gate voltage V_G is shown in Fig. 4(b) with a bias current of 0.4 A for maximum linearity and dynamic range. A biasing network sets the bias gate voltage to 5 V and provides a 50 Ω input impedance $Z_L = R_0 = R_1//R_2$, where $R_1 = R_2 = 100$ Ω. This facilitates the equaliser design since the LED can be considered as a resistive load whose drive current can be controlled by the voltage. A degeneration resistor $R_3 = 680$ mΩ is used to obtain the linear V-I curve shown in Fig. 4(b).
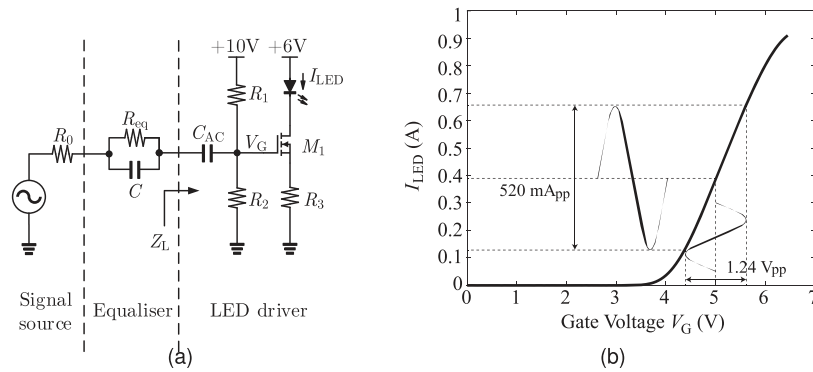
Fig. 4. Driver and pre-equaliser for the LED: (a) schematic and (b) the LED's current I_{LED} vs. gate voltage V_G.

TABLE 1

Design Parameters for Three Types of RC Equalisers

Type	Value	DC SNR loss		System bandwidth with EQ	
		Designed[1]	Measured	Designed[2]	Measured
EQ1	111 Ω//200 pF	6.5 dB	6 dB	15 MHz	18 MHz
EQ2	240 Ω//82 pF	10.6 dB	11 dB	27 MHz	26 MHz
EQ3	510 Ω//42 pF	15.7 dB	15 dB	45 MHz	45 MHz

[1]The designed DC SNR loss is calculated by $20\log\frac{1}{2} - 20\log(\frac{R_0}{2R_0+R_{eq}})$.

[2]The designed system bandwidth with equaliser is calculated by $B_{mod} = \frac{1}{2\pi(2R_0//R_{eq})C}$.
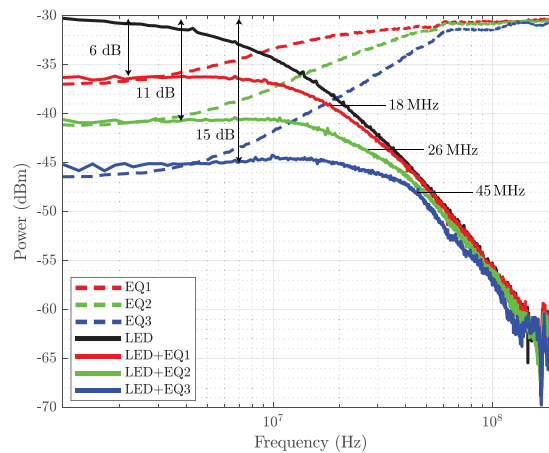
Fig. 5. Frequency response of the LED, equalisers and LED with three equalisers.

3.2 Pre-Equaliser Design

Following the design criterion in (12), we have designed and implemented three types of *RC* equalisers with the design parameters given in Table 1. As predicted, the third equaliser offers the highest bandwidth improvement with the largest DC SNR loss of 15 dB. The measured frequency response of the LED, all three equalisers and the equalised LED are given in Fig. 5.
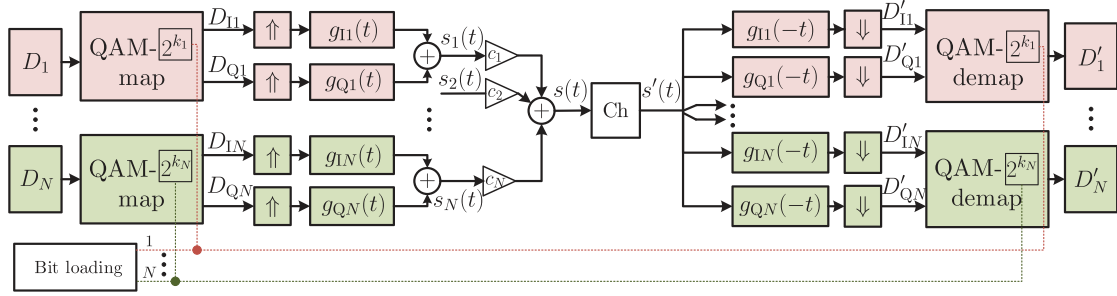
Fig. 6. System block diagram of m-CAP with bit-loading.

4. Multi-Carrier Modulation Scheme: m-CAP With Bit-Loading

To experimentally verify that multi-carrier modulation can achieve higher capacity than analogue equalisers, we have adopted multi-band CAP because of its low implementation complexity. A brief review of m-CAP is provided as follows. Due to the limited space and in order to remain within the focus of the paper, details of m-CAP are not reviewed here and can be found in the literature [9], [26], [27].

CAP is a bandwidth-efficient passband modulation scheme derived from QAM [28], where the carrier and the mixer are embedded into the pulse shaping filter to reduce implementation complexity. The single carrier CAP requires a flat frequency response to obtain low BER, which is achievable within the pass-band of the LED. However, beyond an LED's 3-dB bandwidth, the LED has an attenuation rate of 20 dB per decade [18]. By increasing the number of sub-carriers, the frequency response in each band can be approximated to be flat, which eliminates the need for an equaliser. To increase the system data rate further, each sub-carrier then can be loaded with different orders using bit-loading algorithms.

Fig. 6 shows the system block diagram of m-CAP. At the Tx, a random symbolic sequence D_n is mapped into the QAM-2^{k_n} constellation, where k_n is the bit per symbol loaded onto the n-th sub-carrier at

$$f_n = \frac{2n-1}{2N} B_{\text{mod}}, \tag{20}$$

where $n = 1, \ldots, N$ is the carrier index, and N is the number of sub-carriers. Following constellation mapping, D_n is split into the in-phase branch D_{In} and quadrature branch D_{Qn}.[7] Then D_{In} and D_{Qn} are upsampled and convoluted with the in-phase and quadrature filters of

$$g_{In}(t) = g(t) \sin 2\pi f_n t, \quad g_{Qn}(t) = g(t) \cos 2\pi f_n t \tag{21}$$

to form each sub-carrier CAP signal, which is given by

$$s_n(t) = D_{In} \circledast g_{In}(t) + D_{Qn} \circledast g_{Qn}(t), \tag{22}$$

where

$$g(t) = \frac{\sin[\pi(1-\beta)t/T_s] + 4\beta t/T_s \cos[\pi(1+\beta)t/T_s]}{\pi t/T_s \left[1 - (4\beta t/T_s)^2\right]} \tag{23}$$

is the square-root raised cosine pulse, $0 < \beta < 1$ is the roll-off factor, and $T_s = \frac{1+\beta}{B_{\text{mod}}/N}$ is the symbol period for transmitting D_{In} and D_{Qn}. Finally, all CAP signals are summed up to generate the multi-band signal

$$s(t) = \sum_{n=1}^{N} c_n s_n(t) \tag{24}$$

[7]For square QAM constellations, D_{In} and $D_{Qn} \in \{\pm 1, \pm 3, \ldots, \pm(\sqrt{2^{k_n}} - 1)\}$. For cross QAM constellations, please see [29].
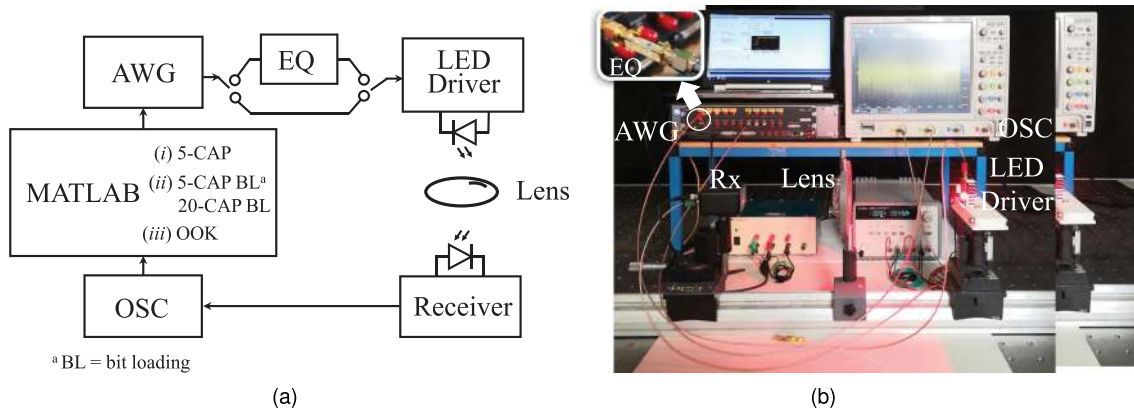
Fig. 7. (a) System block diagram and (b) experimental setup.

where c_n is the coefficients to load equal power onto each band and is given by [29]

$$c_n = \begin{cases} \sqrt{\dfrac{6}{2^{k_n}-1}} & \text{if } k_n \geq 2 \text{ and } k_n \text{ is even,} \\[2mm] \sqrt{\dfrac{6}{\frac{31}{32}2^k-1}} & \text{if } k_n > 3 \text{ and } k_n \text{ is odd,} \\[2mm] \sqrt{2/3} & \text{if } k_n = 3. \end{cases} \tag{25}$$

At the Rx, the received signal $s'(t)$ is convoluted with $2N$ matched filters with the pulse response of $g_{In}(-t)$ and $g_{Qn}(-t)$ followed by downsampling in order to recover D'_{In} and D'_{Qn}. Finally D'_{In} and D'_{Qn} are demapped by QAM-2^{k_n} demodulation modules to recover D'_n, which is compared with D_n to determine the bit error rate (BER).

In bit-loading, the largest QAM order sequence $\{2^{k_n}\}$ for all carriers for a required BER level is determined. In this paper, this process is carried out recursively by offline BER measurement in a symbol-by-symbol manner in order to find the largest constellation for each sub-carrier below a BER of 3.8×10^{-3}.

For bit-loaded m-CAP, the aggregate data rate is[8]

$$R_{\text{total\_BL}} = \sum_{n=1}^{N} k_n \cdot \frac{1}{T_s} = \frac{\overline{k_n}B_{\text{mod}}}{1+\beta}, \tag{26}$$

where $\overline{k_n} = \frac{1}{N}\sum_{n=1}^{N} k_n$ is the average loaded bit-per-symbol.

5. VLC Experimental Setup

Fig. 7 shows the experimental testbed for evaluating the VLC link for the following cases of (i) m-CAP with equaliser; (ii) m-CAP without equaliser but with bit loading; and (iii) OOK with/without equaliser. A set of random symbolic sequences $\{D_n\}$ is used to generate m-CAP waveforms in MATLAB. Then the waveform is uploaded to the arbitrary waveform generator (AWG, M8190 Keysight) to modulate the LED's intensity. At the Rx, a wideband optical receiver (Newport 1601, 1 GHz bandwidth) is used to regenerate the electrical signal, which is captured by a digital oscilloscope (DSO9254, Keysight) for offline processing in the MATLAB domain. The key parameters are given in Table 2. For m-CAP with pre-equalisers, the modulation bandwidth is varied with the equalised

---

[8]Note that the data rate of m-CAP depends only on B_{mod} and $\overline{k_n}$. In other words, the number of sub-carriers does not affect the system data rate if the channel is ideal. For non-ideal channel with non-flat response, enough sub-carriers should be used to let $\overline{k_n}$ approach the average spectrum efficiency.

TABLE 2

Key System Parameters

Parameter	Value
LED	OSRAM, LR W5SM, red, 628 nm, bias current 400 mA
AWG output voltage	675 mVpp[1]
Optical receiver	Newport model 1601, bandwidth 30 kHz 1 GHz, AC gain 700 V/A
Lens	Convex, focal length 15 cm
m-CAP roll-off factor	$\beta = 0.15$
5-CAP without EQ	$B_{\mathrm{mod}} = 10$ MHz, $1/T_s = 1.739$ MBaud/s, $f_n = \{1, 3, 5, 7, 9\}$ MHz
5-CAP with EQ1	$B_{\mathrm{mod}} = 20$ MHz, $1/T_s = 3.478$ MBaud/s, $f_n = \{2, 6, 10, 14, 18\}$ MHz
5-CAP with EQ2	$B_{\mathrm{mod}} = 30$ MHz, $1/T_s = 5.217$ MBaud/s, $f_n = \{3, 9, 15, 21, 27\}$ MHz
5-CAP with EQ3	$B_{\mathrm{mod}} = 50$ MHz, $1/T_s = 8.695$ MBaud/s, $f_n = \{5, 15, 25, 35, 45\}$ MHz
5-CAP with bit loading	$B_{\mathrm{mod}} = 50$ MHz, $1/T_s = 8.695$ MBaud/s, $f_n = \{5, 15, 25, 35, 45\}$ MHz
20-CAP with bit loading	$B_{\mathrm{mod}} = 50$ MHz, $1/T_s = 2.174$ MBaud/s, $f_n = \{1.25 : 2.5 : 48.75\}$ MHz[2]
5-CAP bit pattern	$\{4, 5, 4, 3, 2\}$
20-CAP bit pattern	$\{5, 6, 6, 6, 6, 6, 6, 6, 6, 6, 6, 6, 6, 5, 5, 5, 5, 5, 5\}$

[1]The output voltage is fixed for all tests, representing the output power is limited as stated in constraint 2.The voltage swing also guarantees the LED is modulated within the linear dynamic range shown in Fig. 4(b).
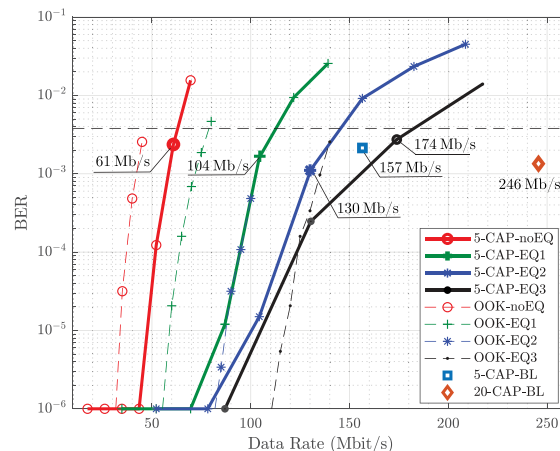[2]The carrier starts from 1.25 MHz and ends at 48.75 MHz with a step size of 2.5 MHz.

Fig. 8. BER vs. the data rate for m-CAP and OOK.

bandwidth, and there is no bit loading. For m-CAP with no pre-equaliser, bit-loading is applied to determine the bit sequence $\{k_n\}$, and a higher number of sub-carriers (i.e., 20) are used to achieve improved performance. This is because employing 5 sub-bands in the stopband of the LED will not satisfy the quasi-flat channel requirement. For comparative purposes, OOK BER performance was also evaluated using the same setup but was estimated from Q-factor measured by the oscilloscope.

6. Results and Discussions

Fig. 8 shows the BER performance as a function of the data rate for 5-CAP with no pre-equaliser, 5-CAP with three pre-equalisers, 5- and 20-CAP with bit loading. For reference, the BER performance of OOK with and without pre-equaliser is also provided. As shown, at a BER of 3.8×10^{-3}, 5-CAP with no EQ (raw LED), EQ1, EQ2 and EQ3 offers data rates of 61, 104, 130 and 174 Mb/s, respectively, which agrees with the previous analysis. In comparison to the equalised systems, 20-CAP using bit loading achieves a data rate of 246 Mb/s, which outperforms all other systems
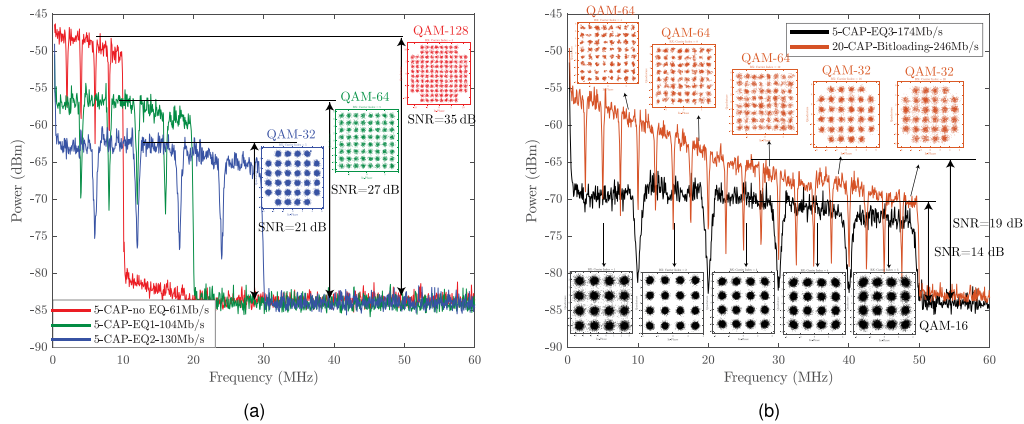
Fig. 9. Measured spectrum of the received signal for (a) 5-CAP with no EQ, EQ1 and EQ2, and (b) 5-CAP with EQ3, and 20-CAP with bit loading using the raw LED. (measured using Keysight spectrum analyser N9010 A).

as predicted. For comparative purposes, Fig. 8 also shows 5-CAP with bit loading achieving a data rate of 157 Mb/s due to the non-flat response in each sub-band caused by the limited number of carriers.

Fig. 9(a) and (b) depict the measured spectrum for 5-CAP with no EQ, EQ1, EQ2 and EQ3, and 20-CAP with bit loading at the highest data rates of 61, 104, 130, 174 and 246 Mb/s, respectively. Also shown are the corresponding constellation diagrams, which demonstrate the quality of data transmission over the links with and without equalisers. From the spectra of the 5-CAP with equalisers, the average SNR is reduced from 35 to 27, 21 and 14 dB with decreased constellation size, thus offering reduced spectrum efficiency. For 5-CAP with EQ3, see Fig. 9(b), the measured SNR[9] is 14 dB, which agrees well with the estimated SNR as highlighted in Fig. 2(b). For 20-CAP with bit loading, the spectrum lies above 5-CAP with EQ3, indicating that for each sub-band a larger constellation can be adopted as shown by the insets in Fig. 9(b). This explains why the raw system with bit loading can offer higher data rates than equalised systems. For comparative purposes, the estimated theoretical capacity of our system with EQ3 in Fig. 2(b) is 235 Mb/s, while our practical system achieved 174 Mb/s. The gap between the predicted and measured data rates might be due to the non-ideal demodulation algorithm and hardware limitation.[10] However, 20-CAP can achieve a data rate of 246 Mb/s, which is higher than the estimated capacity of an equalised system and thus validates our proposed model.

Compared with [3], [10], [13], [22], [23], data rates achieved in this paper is lower because of the following reasons: (i) The TIA receiver has a relatively low gain; (ii) The optics for focusing light on the small photodiode is unable to collect the optical power efficiently; (iii) The maximum modulation bandwidth in our experiment is 50 MHz and can be increased further to achieve higher data rates.

7. Conclusion

We proposed a universal model for the VLC system with analogue pre-equalisers and obtained a pre-equaliser design method for single colour LEDs. From the model, we showed that the pre-equaliser based system can increase the data rate by extending the normalised 3-dB bandwidth

---

[9]The SNR is measured by reading the vertical height from the top of the spectrum haystack down to the noise floor. This method actually measures $(1 + \text{SNR})$, which requires a correction to back out the noise underlying the signal [30] Here we neglect this effect because of high SNR.

[10]The received signal is captured using an oscilloscope for offline processing. Due to the high analogue frontend bandwidth of the oscilloscope, the noise floor can be higher and results in lower SNR than measured by the spectrum analyser.

at the cost of SNR penalties. We also showed that VLC with multi-carrier modulation and bit-loading offered higher data rates than the equalised system because of absence of SNR penalties and higher spectrum efficiency. We developed an experimental test-bed to verify the analysis and results showed that for VLC with equalisers the data rate increased from 61 to 174 Mb/s when the equalised bandwidth was extended from 7.5 MHz to 48 MHz. In comparison to equalised VLC systems, the raw LED based VLC system achieved a data rate of 246 Mb/s by using 20-CAP with bit loading. The analogue pre-equaliser can be used as an efficient method to improve the system data rate with low implementation complexity. However, for multi-carrier modulation with bit-loading, if the analogue pre-equaliser introduces a significant SNR loss, as in this work, it may be unnecessary as it will substantially reduce the number of bits-per-symbol available on each subcarrier, which is detrimental to overall system performance.

References

[1] Z. Ghassemlooy, W. Popoola, and S. Rajbhandari, *Optical Wireless Communications: System and Channel Modelling with MATLAB*, 2nd ed. Boca Raton, FL, USA: CRC Press, 2019.

[2] M. Uysal, C. Capsoni, Z. Ghassemlooy, A. Boucouvalas, and E. Udvary, *Optical Wireless Communications: An Emerging Technology*. Berlin, Germany: Springer, 2016.

[3] Y.-C. Chi *et al.*, "Phosphorous diffuser diverged blue laser diode for indoor lighting and communication," *Sci. Rep.*, vol. 5, 2015, Art. no. 18690.

[4] F. Zafar, M. Bakaul, and R. Parthiban, "Laser-diode-based visible light communication: Toward gigabit class communication," *IEEE Commun. Mag.*, vol. 55, no. 2, pp. 144–151, Feb. 2017.

[5] C.-T. Tsai, C.-H. Cheng, H.-C. Kuo, and G.-R. Lin, "Toward high-speed visible laser lighting based optical wireless communications," *Prog. Quantum Electron.*, vol. 67, 2019, Art. no. 100225.

[6] G. Stepniak, M. Schppert, and C. Bunge, "Advanced modulation formats in phosphorous LED VLC links and the impact of blue filtering," *J. Lightw. Technol.*, vol. 33, no. 21, pp. 4413–4423, Nov. 2015.

[7] E. F. Schubert, *Light-emitting Diodes*, 3rd ed. Google Books Online, 2018.

[8] P. A. Haigh *et al.*, "Exploiting equalization techniques for improving data rates in organic optoelectronic devices for visible light communications," *J. Lightw. Technol.*, vol. 30, no. 19, pp. 3081–3088, Oct. 2012.

[9] P. A. Haigh *et al.*, "A multi-CAP visible-light communications system with 4.85-b/s/Hz spectral efficiency," *IEEE J. Sel. Areas Commun.*, vol. 33, no. 9, pp. 1771–1779, Sep. 2015.

[10] N. Chi, Y. Zhou, J. Shi, Y. Wang, and X. Huang, "Enabling technologies for high speed visible light communication," in *Proc. Opt. Fiber Commun. Conf.*, (OSA Technical Digest (online)), 2017, Paper. Th1E.3.

[11] H. L. Minh *et al.*, "100-Mb/s NRZ visible light communications using a postequalized white LED," *IEEE Photon. Technol. Lett.*, vol. 21, no. 15, pp. 1063–1065, Aug. 2009.

[12] N. Fujimoto and S. Yamamoto, "The fastest visible light transmissions of 662 Mb/s by a blue led, 600 Mb/s by a red led, and 520 Mb/s by a green led based on simple OOK-NRZ modulation of a commercially available RGB-type white LED using pre-emphasis and post-equalizing techniques," in *Proc. Eur. Conf. Opt. Commun.*, 2014, pp. 1–3.

[13] X. Huang, Z. Wang, J. Shi, Y. Wang, and N. Chi, "1.6 Gbit/s phosphorescent white LED based VLC transmission using a cascaded pre-equalization circuit and a differential outputs PIN receiver," *Opt. Exp.*, vol. 23, no. 17, pp. 22 034–22 042, 2015.

[14] H. Li, X. Chen, J. Guo, and H. Chen, "A 550 Mbit/s real-time visible light communication system based on phosphorescent white light LED for practical high-speed low-complexity application," *Opt. Express*, vol. 22, no. 22, pp. 27 203–27 213, 2014.

[15] O. J. Zobel, "Theory and design of uniform and composite electric wave-filters," *Bell Syst. Tech. J.*, vol. 2, no. 1, pp. 1–46, 1923.

[16] H. W. Bode, *Network Analysis and Feedback Amplifier Design*. New York, NY, USA: D. van nostrand company, 1945.

[17] R. Thatch, "A constant-resistance bridged-T equalizer using transmission-line elements," *IEEE Trans. Circuit Theory*, vol. CT-20, no. 5, pp. 577–580, Sep. 1973.

[18] X. Li, Z. Ghassemlooy, S. Zvanovec, M. Zhang, and A. Burton, "Equivalent circuit model of high power LEDs for VLC systems," in *Proc. 2nd West Asian Colloquium Opt. Wireless Commun.*, 2019, pp. 90–95.

[19] H. Li, X. Chen, J. Guo, Z. Gao, and H. Chen, "An analog modulator for 460 Mb/s visible light data transmission based on OOK-NRZ modulation," *IEEE Wireless Commun.*, vol. 22, no. 2, pp. 68–73, Apr. 2015.

[20] C. E. Shannon, "Communication in the presence of noise," *Proc. IRE*, vol. 37, no. 1, pp. 10–21, Jan. 1949.

[21] J.-Y. Sung, C.-W. Chow, and C.-H. Yeh, "Is blue optical filter necessary in high speed phosphor-based white light LED visible light communications?" *Opt. Express*, vol. 22, no. 17, pp. 20 646–20 651, 2014.

[22] X. Huang *et al.*, "2.0-gb/s visible light link based on adaptive bit allocation ofdm of a single phosphorescent white led," *IEEE Photon. J.*, vol. 7, no. 5, Oct. 2015, Art no. 7904008.

[23] F. M. Wu *et al.*, "Performance comparison of OFDM signal and CAP signal over high capacity RGB-LED-based WDM visible light communication," *IEEE Photon. J.*, vol. 5, no. 4, pp. 7 901 507–7 901 507, Aug. 2013.

[24] C. DeCusatis, *Handbook of Fiber Optic Data Communication: A Practical Guide to Optical Networking*. New York, NY, USA: Academic, 2013.

[25] R. H. Saul, T. P. Lee, and C. A. Burrus, *Light-emitting-diode Device Design*, vol. 2. Amsterdam, The Netherlands: Elsevier, 1985, pp. 193–237.

[26] P. A. Haigh *et al.*, "Multi-band carrier-less amplitude and phase modulation for bandlimited visible light communications systems," *IEEE Wireless Commun.*, vol. 22, no. 2, pp. 46–53, Apr. 2015.

[27] M. I. Olmedo *et al.*, "Multiband carrierless amplitude phase modulation for high capacity optical data links," *J. Lightw. Technol.*, vol. 32, no. 4, pp. 798–804, Feb. 2014.

[28] D. Falconer, "Carrierless AM/PM," Bell Laboratories, New Providence, NJ, USA, Bell Laboratories Technical Memorandum, Tech. Rep., 1975.

[29] J. M. Cioffi, *Signal Processing and Detection*, 2018. [Online]. Available: http://www.stanford.edu/group/cioffi/book/chap1.pdf

[30] R. Hranac, "Digital transmission: Carrier-to-noise ratio, signal-to-noise ratio, and modulation error ratio," Broadcom Corporation and Cisco Systems, 2006.